CHEMISTRY
A EUROPEAN JOURNAL

DOI: 10.1002/chem.200802294

Intramolecular Metal–Fluorocarbon Coordination, C−F Bond Activation and Lanthanoid–Fluoride Clusters with Tethered Polyfluorophenylamide Ligands

Glen B. Deacon,* Craig M. Forsyth, Peter C. Junk,* and Jun Wang[a]

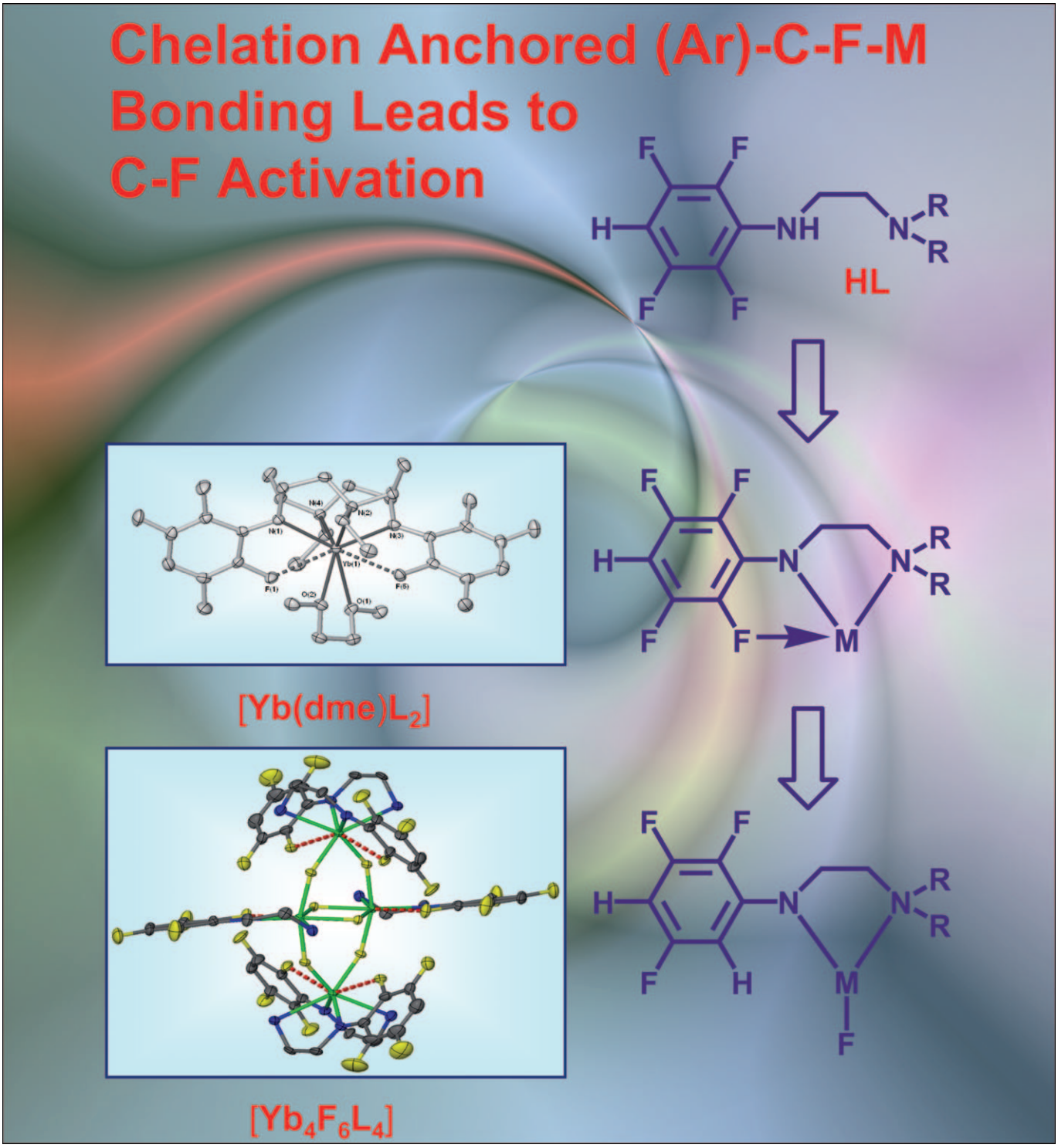

Abstract: Metalation of either *N*,*N*-diethyl- or *N*,*N*-dimethyl-*N*′-2,3,5,6-tetrafluorophenylethane-1,2-diamines (HL **1a**, **1b** respectively) with [M{N(SiMe$_3$)$_2$}] (M = Na, K) or [Yb{N(SiMe$_3$)$_2$}$_2$(thf)$_2$] yielded the metal–amido compounds [Na(L)] (**2a**), [K(L)] (**3a**) and [Yb(L)$_2$(thf)$_2$] (**4a**, **4b**). The Yb complexes were also synthesised by redox transmetalation/ligand exchange from Yb, Hg(C$_6$F$_5$)$_2$ and HL in THF or **4a** from a reaction of **3a** with YbI$_2$ in THF. In the presence of *N*,*N*,*N*′,*N*′-tetramethyl-1,2-ethanediamine (TMEDA) the complexes **2a** and **3a** yielded [Na(L)$_2$Na(tmeda)] (**5a**) and [K$_2$(L)$_2$(tmeda)$_2$] (**6a**), respectively, as crystalline compounds, whilst crystallisation of **4a** from DME gave [Yb(L)$_2$(dme)] (**7a**). Their structures have chelating metal–amide and NR$_2$ donors and additional intramolecular M-F-C connectivity with relatively short bond lengths (Na–F 2.65–3.00 Å; K–F 2.70–3.00 Å; Yb–F 2.56 Å). The Yb complexes undergo C–F activation in solution forming [Yb$_4$(L)$_6$F$_6$] (**8a**, **8b**). The connectivity of [Yb$_4$(L)$_6$F$_6$], as shown by the X-ray structures, comprised a circular Yb$_4$(μ-F)$_4$ periphery with two opposing Yb centres having either one L ligand and a Yb$_2$(μ-F)$_2$ bridge or two L ligands. Each polyfluorophenylamide exhibits additional intramolecular Yb-F-C coordination from one of the *ortho*-F atoms resulting in seven or eight coordinate Yb centres. An attempt to synthesise **4a** by redox transmetalation/ligand exchange using Hg(C≡CPh)$_2$ as the mercury reagent gave [Yb$_4$(O)$_2$(L)$_4$(C≡CPh)$_4$(thf)$_2$]·THF (**9a**·THF), most likely as a result of oxidation of the initially formed product.

Keywords: alkali metals · C–F activation · fluorinated ligands · N ligands · ytterbium

Introduction

An exciting recent development in rare-earth-metal–organic chemistry is the observation of bonds between fluorine atoms of polyfluoroaryl groups and metal atoms (C(Ar)-F-Ln).[1–16] These range from agostic interactions (ca. 3.0 Å) to quite strong bonds (ca. 2.5 Å). In most cases the polyfluoroaryl group is coordinated both through fluorine and another donor atom, for example, 1) carbon (C,F bridging[1] and C,F chelating[2–5]) in polyfluorophenyl–rare-earth compounds, 2) nitrogen in polyfluorophenylamides,[6–8] 3) oxygen in polyfluorophenolates[9] and 4) sulfur in polyfluorothiolates.[10–12] In addition, B(C$_6$F$_5$)$_4^-$ and related anions can act as C(Ar)-F-Ln donors, often chelating through two fluorine atoms.[13–15] Even discrete fluorine-bonded complexes between [Sc(C$_5$Me$_5$)$_2$]$^+$ and fluorobenzene or 1,2-difluorobenzene have been characterised as BPh$_4^-$ salts,[14] whilst the encapsulation of La^{3+} in a cage with polyfluoroarene, N(amine) and O(ether) donor atoms has closer interactions with F than O or N.[16] (There is also related structural chemistry involving fluoroalkyl groups.[17,18]) Such complexes are poised for C–F activation, since the very strong C–F bonds[19,20] are weakened by coordination.[16] Indeed it has been shown that S,F-chelated [Sm(SC$_6$F$_5$)$_3$] yields SmF$_3$ on heating[11] and C,F-chelated [Ce(C$_5$H$_2$-*t*Bu$_3$-1,2,4)$_2$C$_6$F$_5$] decomposes into the corresponding fluoride and tetrafluorobenzyne.[4,5] Other cases of lanthanoid induced C–F activation[21] involve actual[22] or postulated[23–25] polyfluorophenyl– or polyfluorobenzoato–lanthanoid complexes[26] that plausibly form C(Ar)-F-Ln interactions as a step in activation. In many cases, lanthanoid-induced C–F activation leads to the formation of heteroleptic fluorides,[4,19,21–25,27] [Ln(L)$_2$F], [Ln(L)F$_2$], or more complex species including cages and rings.[19,22,23,27a,c] Other examples of these compounds have been made by selective deprotonation of tris(cyclopentadienyl)lanthanoids[28] and by Sn–F[29] and Pb–F[30] activation, but rare earth heteroleptic fluorides remain a limited class. Their existence is of considerable interest given the potential for rearrangement into the corresponding highly stable and insoluble LnF$_3$ compounds. In this paper, we report a series of ytterbium(II) polyfluoroorganoamides with strong C(Ar)-F-Yb coordination and that undergo C–F activation to give the fluoro(organoamido)lanthanoid cages [Yb$_4$F$_6$(L)$_6$] (L = *p*-HC$_6$F$_4$N(CH$_2$)$_2$NR$_2$; R = Et or Me). In each of the ytterbium complexes, as well as in the alkali metal derivatives prepared as metathesis reagents, the *N*,*N*-dialkyl-*N*′-2,3,5,6-tetrafluorophenyl-ethane-1,2-diaminate(1−) ligands act as tridentate *o*-F,N,N′ ligands and show strong C(Ar)-F-M binding.

Results and Discussion

N,*N*-Dialkyl-*N*′-2,3,5,6-tetrafluorophenylethane-1,2-diaminate(1−) ligands were first reported in the platinum(II) complexes [Pt(L)X(py)] (X = Cl, Br, I) in which the ligands were assembled in situ by a combination of decarboxylation and nucleophilic substitution processes.[31a,b] The ligand HL (**1a**, **1b**) can be more conveniently prepared from the appropriate *N*,*N*-dialkylethane-1,2-diamine and C$_6$F$_5$H heated to reflux in EtOH (Scheme 1).[31c] Subsequent metalation reactions with [M{N(SiMe$_3$)$_2$}] (M = Na, K) or [Yb{N(SiMe$_3$)$_2$}$_2$(thf)$_2$] in THF or PhMe/THF mixtures readily yielded the corresponding metal complexes [M(L)] (R = Et; M = Na **2a**, K **3a**) or [Yb(L)$_2$(thf)$_2$] (R = Et **4a**, R = Me **4b**) in good yields (Scheme 1). The Yb complexes were also synthesised by redox transmetalation/ligand exchange reactions

[a] Prof. Dr. G. B. Deacon, Dr. C. M. Forsyth, Prof. Dr. P. C. Junk, Dr. J. Wang
School Of Chemistry, Monash University
Clayton VIC 3800 (Australia)
Fax: (+61) 399054597
E-mail: glen.deacon@sci.monash.edu.au

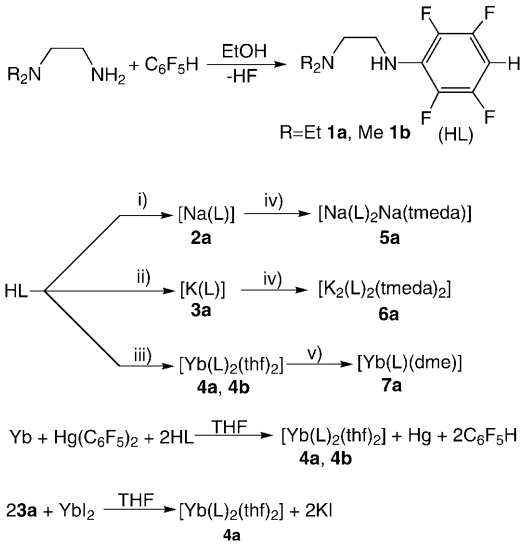

Scheme 1. Synthesis of ligands (HL) and metal complexes i) [Na{N(SiMe$_3$)$_2$}], THF; ii) [K{N(SiMe$_3$)$_2$}], THF; iii) [Yb{N(SiMe$_3$)$_2$}$_2$(thf)$_2$], THF; iv) TMEDA, PhMe; v) DME.

of HL (**1a** or **1b**) with Yb metal and $Hg(C_6F_5)_2$ in THF and **4a** by metathesis from **3a** and YbI_2 (Scheme 1). The Na and K derivatives were obtained as powders insoluble in PhMe and without coordination by additional donors (e.g., THF). However, addition of *N*,*N*,*N*′,*N*′-tetramethyl-1,2-ethanediamine (TMEDA) gave the crystallisable complexes [Na(L)$_2$Na(tmeda)] (**5a**) and [K$_2$(L)$_2$(tmeda)$_2$] (**6a**; Scheme 1). Analogously, the ytterbium complex **4a**, gave [Yb(L)$_2$(dme)] (**7a**) when crystallised from DME.

The metal complexes were characterised spectroscopically and single-crystal X-ray structures were determined for **5a**, **6a** and **7a**. IR spectra showed absorptions attributable to the ligands and the ν(N–H) frequency was absent, consistent with deprotonation and coordination to the metal. For the Na and K complexes **2a** and **3a**, there were no spectroscopic features attributable to the presence of residual solvent (THF) and the compositions were confirmed by elemental analyses. The presence of TMEDA in **5a** and **6a** was confirmed by the ^{1}H NMR spectra, but the elemental analyses were consistently low in the percentage of C present, attributable to partial loss of TMEDA on standing. The analyses corresponded to the compositions [Na$_4$(L)$_4$(tmeda)] and [K$_4$(L)$_4$(tmeda)$_3$]. Similarly, the composition of the ytterbium(II) complexes **4a** and **4b** was established by their ^{1}H NMR spectra, but the elemental analyses indicated loss of one THF molecule. In contrast, **7a** gave satisfactory elemental analyses. The room-temperature ^{171}Yb NMR data for **4a** (δ=490 ppm in C_7D_8) and **7a** (δ=389 ppm in C_6D_6) are in the region observed for the eight coordinate complex [Yb(Ph$_2$pz)$_2$(dme)$_2$] (Ph$_2$pz=3,5-diphenylpyrazolate)(δ=480 ppm).[32a] However, the resonances of **4a** were markedly solvent- and temperature-dependent. Either cooling or addition of THF caused an upfield shift (δ=405 ppm at −80 °C, δ=398 ppm in 1:1 C_6D_6/THF) indicative of an increase in the coordination number. A progressive decrease in ^{171}Yb NMR shifts with increasing coordination number has been observed previously for series of complexes in which the anionic ligand is the same or closely related.[32b,c] The similarity of the chemical shift of **4a** at low temperature and in the presence of THF with that of the DME complex **7a** suggests that the coordinated THF is dissociatively labile (Scheme 2), consistent with the analytical data. Eight coordinate ytterbium is indicative of tridentate (N,N′,F) binding of the polyfluorophenylamide ligands as observed in the solid-state (below).

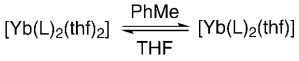

Scheme 2.

The room-temperature ^{19}F NMR spectra of complexes **2a**, **3a**, **4a**, **4b**, **5a**, and **6a** showed only two resonances for the *ortho* (ca. δ=−169(±4) ppm) and *meta* (ca. δ=−148(±3) ppm) fluorine nuclei. These values show a distinct high-field shift (ca. 17 ppm) for the *ortho*-fluorine resonance when compared with those for the platinum(II) complex *trans*-[Pt(N(R)CH$_2$CH$_2$NMe$_2$))Cl(py)] (R=C$_6$F$_4$-*p*-H; δ=−144.4 and −152.1 ppm).[31a] In contrast, the ytterbium complex **7a** showed four separate resonances (in an approximately 1:1:1:1 ratio) at −142.9 −148.8, −162.2 and −166.6 ppm which coalesced to two broad signals at −145.8 and −164.3 ppm on heating above 50 °C. Similarly, cooling samples of **3a** and **4a** enabled resolution into four separate resonances at −70 °C. These data are consistent with a fluxional system in which restricted rotation of the N-C$_6$F$_4$H ring leads to a lower symmetry environment. The small chemical-shift separation of the two *ortho*- and *meta*-F resonances (ca. 4 ppm) may be attributed to M···F–C interactions that are observed in the crystal structures (see below) and would lead to inequivalent fluorine atoms. No Yb–F coupling[33] was observed in ^{171}Yb NMR spectra, although at −80 °C the resonance for **4a** was very broad (ca. 300 Hz) and showed evidence of a shoulder.

The single-crystal X-ray structures of one example each of the Na, K, and Yb complexes were determined to clarify the bonding of these amide ligands to the metals. The Na complex **5a** (Figure 1) is composed of a dinuclear arrangement with the two Na centres bridged by the amido N atoms with the pendant CH$_2$CH$_2$NEt$_2$ arms both chelating to Na(1). The tmeda ligand binds to Na(2). The corresponding complex with the larger K cation (Figure 2) shows a symmetrical dinuclear structure also with bridging amido N atoms, but with one of the chelating CH$_2$CH$_2$NEt$_2$ arms and one bidentate tmeda coordinating to each K centre. These structural motifs have previously been observed in complexes with an alkoxysilylamido ligand, for example, [Na{N(SiMe$_3$)(SiMe$_2$O*t*Bu)}$_2$Na(bpy)] (Type A) and [K$_2${N(SiMe$_3$)(SiMe$_2$O*t*Bu)}$_2$(bpy)$_2$] (Type B).[34a] In the current structures the bridging M–N(amido) distances (Table 1) are marginally shorter (Na) or shorter (K) than observed in the

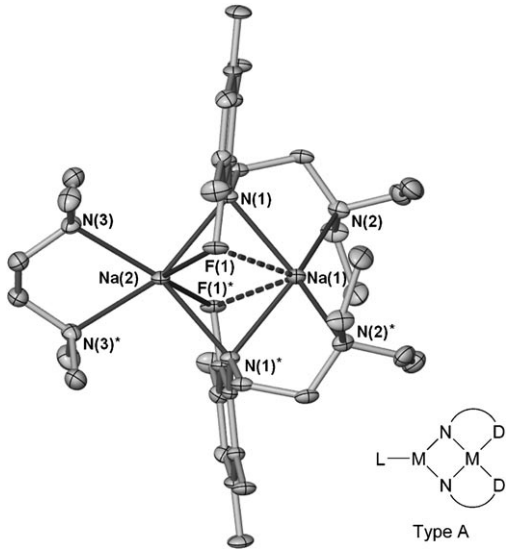

Figure 1. Molecular diagram of $[Na(p\text{-}HC_6F_4N(CH_2)_2NEt_2)_2Na(tmeda)]$ (**5a**) as shown with 50% thermal ellipsoids and hydrogen atoms omitted for clarity (* denotes symmetry generated atom). Inset: schematic representation of general structural motif L = bidentate ligand.

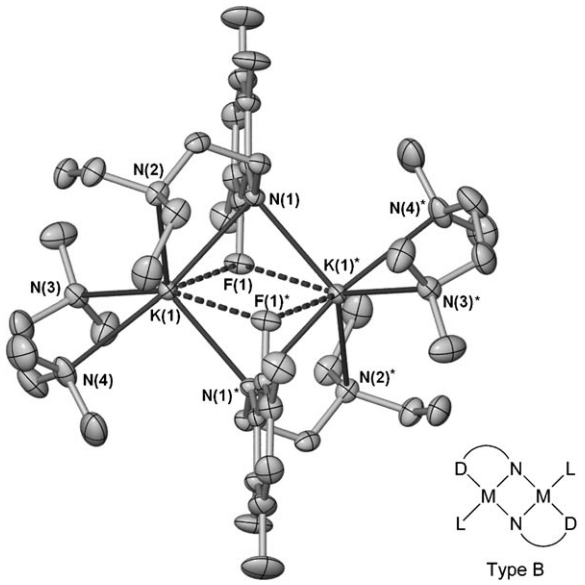

Figure 2. Molecular diagram of $[K(p\text{-}HC_6F_4N(CH_2)_2NEt_2)(tmeda)]_2$ (**6a**) as shown with 50% thermal ellipsoids and hydrogen atoms omitted for clarity (* denotes symmetry generated atom). Inset: schematic representation of general structural motif, L = bidentate ligand.

alkoxysilylamido complexes (Na 2.450(6), 2.451(7); K 2.853(4), 2.892(3) Å),[33] whereas the M–N(amine) bond lengths are typical for M–tmeda complexes, for example, Na 2.511(2), 2.510(6) Å and K 2.824(2), 2.906(3) Å in six coordinate $[M_2(\mu\text{-}NMePy)_2(tmeda)_2]$.[34b]

In both the Na and K structures, each metal centre also interacts with one *ortho*-fluorine atom of the polyfluorophenylamide ligands. The M–F contacts form a bridge between the two metal atoms, approximately perpendicular to the M-(μ-N)$_2$-M plane. For the Na derivative **5a**, one Na–F distance to Na(2) is only 0.15 Å longer than the Na–N(tmeda) distances. Reported Na–F(Ar) contacts lie in the range 2.298–2.995 Å,[35a] with the closest analogue (in terms of chelate ring size) being $[\{Na\{(C_6H_4\text{-}o\text{-}F)NCN(C_6H_4\text{-}o\text{-}F)\}(OEt_2)\}_2]$, 2.345(2) Å.[35b] With the Na–F contacts included, the two sodium environments are six coordinate and form distorted trigonal prisms, sharing a rectangular face. In **6a** the K_2–μF interactions are more symmetrically disposed with distances within the range reported for previous examples of this type of interaction (e.g., $[K\{(C_6H_4\text{-}o\text{-}F)NCN(C_6H_4\text{-}o\text{-}F)\}]_\infty$ 2.805(4), 3.030(4) Å).[35b] Overall, the K coordination number is seven, consistent with the larger ionic radius than Na,[36] with the donor atoms having an irregular geometry.

Table 1. Selected bond lengths [Å] in $[Na(L)_2Na(tmeda)]$ (**5a**), $[K_2(L)_2(tmeda)_2]$ (**6a**) and $[Yb(L)_2(dme)]$ (**7a**) (L = p-$HC_6F_4N(CH_2)_2NEt_2$).

5a		**6a**		**7a**	
Na(1)–N(1)	2.410(2)	K(1)–N(1)	2.782(2)	Yb(1)–N(1)	2.428(3)
Na(2)–N(1)	2.429(2)	K(1)–N(1)*[a]	2.792(2)	Yb(1)–N(3)	2.436(3)
Na(1)–N(2)	2.558(2)	K(1)–N(2)	2.996(2)	Yb(1)–N(2)	2.729(3)
Na(2)–N(3)	2.518(2)	K(1)–N(3)	2.973(2)	Yb(1)–N(4)	2.728(3)
		K(1)–N(4)	2.885(2)	Yb(1)–O(1)	2.560(3)
				Yb(1)–O(2)	2.588(3)
Na(1)–F(1)	3.000(2)	K(1)–F(1)	2.867(1)	Yb(1)–F(1)	2.558(2)
Na(2)–F(1)	2.653(1)	K(1)–F(1)	3.009(1)	Yb(1)–F(5)	2.560(2)

[a] Symmetry operator *: $-x+1, -y+2, -z+1$.

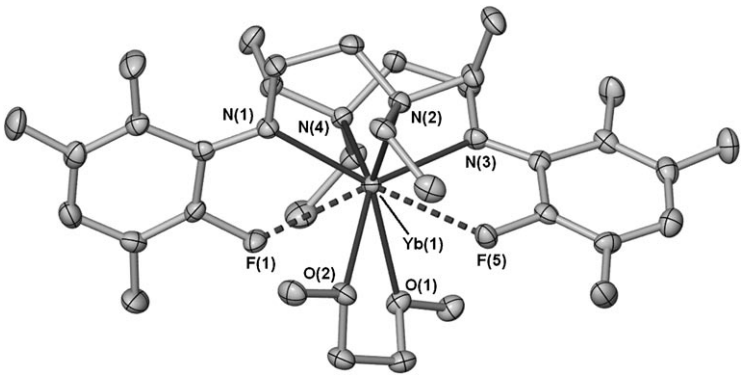

Figure 3. Molecular diagram of $[Yb(p\text{-}HC_6F_4N(CH_2)_2NEt_2)_2(dme)]$ (**7a**) shown with 50% thermal ellipsoids and hydrogen atoms omitted for clarity. The Yb-*o*-F contacts are indicated by dashed bonds.

In contrast to **5a** and **6a**, the Yb complex **7a** is mononuclear (Figure 3), with a distorted trigonal prismatic geometry (N(1), N(2), O(2) and N(3), N(4), O(1) comprising the trigonal faces). The Yb–N(amido) and Yb–N(amine) moieties show the expected shorter Yb–N bonds for the negatively charged amido nitrogen atoms (Table 1). This contrasts binding of delocalised NCN ligands, such as amidinates, which show symmetrical, but marginally longer, Yb–N distances (e.g., in six-coordinate $[Yb(L)_2(thf)_2]$, L = PhC(NSiMe$_3$)$_2$ 2.468(2), 2.478(2) Å).[37] A significant feature of **7a** is the observation of ytterbium–fluorine contacts to one

of the *ortho*-F atoms on the C_6F_4-*p*-H substituent of each ligand. These contacts cap two of the rectangular faces of the Yb trigonal prism and the Yb–F distances are comparable to the Yb–O bond lengths of the O(dme) donors and shorter than the Yb–N(amine) distances. Corroborating the description of these Yb–F interactions as genuine metal coordination bonds, the Yb–N and Yb–O bond lengths in **7a** are generally longer than for an analogous six-coordinate complex with bidentate (N,O) amido ligands (e.g., $[Yb\{N(SiMe_3)(C_6H_4\text{-}o\text{-}OMe)\}_2(dme)]$ Yb–N 2.353(4), Yb–O 2.40(1)–2.55(1) Å),[38] consistent with an approximate 0.10 Å increase in ionic radii for eight coordinate Yb.[36] The most closely analogous lanthanoid organoamide complex with Ln–F interactions is $[Sm\{N(SiMe_3)(C_6F_5)\}_3]$ in which each ligand has one close Sm^{III}–F contact in the range 2.561–2.587 Å.[6] Related Eu^{II} complexes with XC_6F_5 (X = O, S) ligands have significantly longer bonds (e.g., $[Eu_3(OC_6F_5)_6(dme)_4]$, 2.928(2), 3.013(2) Å and $[Eu(SC_6F_5)_2(thf)_2]_\infty$ 3.006(6) Å).[9,11]

The ytterbium(II) complexes **4a** and **4b** are thermally unstable. This was initially observed when the crude materials from evaporation of filtered solutions from redox transmetalation/ligand exchange syntheses of **4a** or **4b** (see Scheme 1) were dissolved in PhMe and allowed to stand at room temperature for several weeks. After this time, pale yellow crystals had deposited that were shown to be the ytterbium(III) fluoride cluster compounds $[Yb_4F_6(L)_6]$ **8a** and **8b**·4PhMe (Scheme 3). Crystals of **8b**·2THF were also obtained direct-

$$4\,[Yb(L)_2(thf)_2] \xrightarrow{PhMe} [Yb_4(L)_6F_6] + \text{defluorinated ligands}$$

Scheme 3. Synthesis of the fluoride cluster complex $[Yb_4(L)_6F_6]$ **8a/8b** from the Yb^{II} precursors **4a/4b**.

ly from the reaction solution. NMR scale studies of the decomposition of freshly isolated and pure **4a** (in C_6D_6) or **4b** (in PhMe/C_7D_8), showed complete disappearance of the ^{19}F NMR signals for these compounds over time. In the case of **4b**, growth of four new resonances at $\delta = +103.1$, -30.6, -130.5, and -182.3 ppm in an approximate ratio of 1:2:6:6 were observed. Accompanying these changes, crystals of **8a**·C_6D_6 or **8b**·4PhMe formed in the NMR tube and these were characterised by X-ray crystallography (see below). Subsequently, larger scale (1 mmol) conversions of **4b**→**8b** were performed in PhMe or PhMe/perfluorohexane and gave **8b**·4PhMe in good yield (Scheme 3). The ^{19}F NMR resonances observed during the decomposition of **4b** (see above) were broad and the wide chemical shift range is consistent with the presence of a paramagnetic ytterbium(III) centre. The two more intense resonances, $\delta = -130.5$ and -182.3 ppm, are reasonably assigned to the *ortho*- and *meta*-fluorine atoms of the ligands by comparison with data for $[Ln(SC_6F_5)_3(solv)_x]$ solv = thf, $x = 3$; solv = py, x = 4 ($\delta^{19}F = -96.3$ to -132.5 and -148.4 to -179.9 ppm for Ln = Ce, Ho, Er, Sm, Yb).[10] The remaining two peaks may therefore represent ytterbium(III)–fluoride species. Comparable data for lanthanoid fluorides are rare, but $[La(L)_2F(thf)]$ ($\delta^{19}F$ +150.2 ppm) and $[Sm(L)_2F(thf)$ ($\delta^{19}F = -24.8$ ppm) [L = $(C_6H_3\text{-}2,6\text{-}iPr_2)NC(H)N(C_6H_3\text{-}2,6\text{-}iPr_2)$] have been reported,[24] and are in the region of the current data. Unfortunately, once crystallised, both **8a** and **8b** were insoluble in THF and no satisfactory NMR spectra could be obtained for the isolated materials and it is possible that the above data are for an intermediate species.

Crystal structures were obtained for both complexes, as varying different solvates for example, **8a** (without lattice solvent), **8a**·C_6D_6, **8b**·2thf, **8b**·4PhMe, but the dried bulk compounds gave satisfactory microanalyses for the solvent free compositions **8a** or **8b**. The structures are all closely similar (Table 2), each comprising a centrosymmetric mole-

Table 2. Selected bond lengths [Å] in $[Yb_4(L)_6F_6]$ complexes (L = *p*-$HC_6F_4N(CH_2)_2NEt_2$ **8a**, L = *p*-$HC_6F_4N(CH_2)_2NMe_2$ **8b**).[a]

	8a	**8a**·C_6D_6	**8b**·2THF	**8b**·4PhMe
Yb(1)–N(1)	2.301(4)	2.297(10)	2.309(5)	2.284(5)
Yb(1)–N(3)	2.285(4)	2.292(9)	2.294(4)	2.307(5)
Yb(2)–N(5)	2.279(4)	2.269(9)	2.311(5)	2.303(5)
Yb(1)–N(2)	2.642(4)	2.629(9)	2.549(5)	2.549(5)
Yb(1)–N(4)	2.601(4)	2.652(9)	2.559(5)	2.568(5)
Yb(2)–N(6)	2.511(4)	2.525(10)	2.450(4)	2.456(5)
Yb(1)–F(1)	2.489(3)	2.486(7)	2.511(3)	2.503(3)
Yb(1)–F(5)	2.504(3)	2.490(7)	2.491(3)	2.490(3)
Yb(2)–F(9)	2.555(3)	2.511(7)	2.519(3)	2.468(3)
Yb(1)–F(13)	2.162(2)	2.183(5)	2.201(3)	2.191(3)
Yb(1)–F(15)*[a]	2.190(2)	2.165(5)	2.176(3)	2.187(3)
Yb(2)–F(13)	2.158(2)	2.165(5)	2.162(3)	2.148(3)
Yb(2)–F(14)	2.173(2)	2.175(6)	2.170(3)	2.169(3)
Yb(2)–F(14)*[a]	2.169(2)	2.169(6)	2.177(3)	2.167(3)
Yb(2)–F(15)	2.150(2)	2.164(5)	2.142(3)	2.151(3)

[a] Atom labelling corresponding to that in Figure 5 is the same for all complexes. Symmetry operators *: **8a**: $-x+1$, $-y+1$, $-z+1$; **8a**·C_6D_6: $-x+3/2$, $-y+1/2$, $-z+1$; **8b**·2THF: $-x+1$, $-y+1$, $-z+1$; **8b**·4PhMe $-x$, $-y$, $-z$.

cule with four ytterbium centres, two with one L ligand coordinated and two with two *N*,*N*-dialkyl-*N*′-2,3,5,6-tetrafluorophenylethane-1,2-diaminate(1−) ligands (see for example **8b**·4PhMe in Figure 4). At the core of the molecule, a double fluoride bridged dinuclear $\{(L)Yb(\mu\text{-}F)_2Yb(L)\}$ unit is capped, above and below, by a $\{(L)_2Yb(\mu\text{-}F)_2\}$ moiety through fluoride bridging (Figure 4, inset). Although not observed previously for lanthanoids, this type of fluoride-bridged metal array is present in tetranuclear $[\{TiCpF_3\}_4]$,[39] as well as in heterobimetallic fluorides $[\{MCp^*(Me)\}_2(AlMe_2)_2F_6]$·PhMe (M = Ti, Zr, Hf, the Group 4 metals occupying the two central metal sites).[40] As with the Na, K and Yb^{II} complexes above, the *N*,*N*-dialkyl-*N*′-2,3,5,6-tetrafluorophenylethane-1,2-diaminate(1−) ligands are each bound to Yb in a distinctly tridentate fashion through the two N and one of the *o*-F atoms (Figure 4 inset).

With the Yb–F(ligand) contacts included, Yb(1) is eight coordinate with a bi-capped trigonal prismatic coordination geometry, N(1), N(2), F(13) and N(3), N(4), F(15) forming the triangular faces with F(1) and F(5) as the capping atoms.

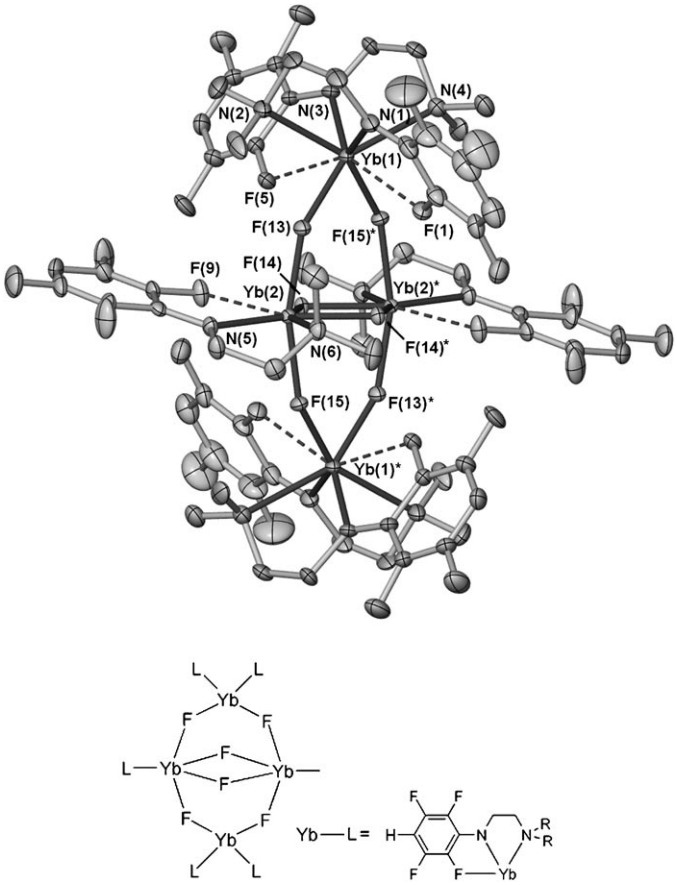

Figure 4. Molecular diagram (and schematic representation—inset) of $[Yb_4(L)_6F_6]$ (L = *p*-$HC_6F_4N(CH_2)_2NMe_2$; **8b**·4PhMe) shown with 50% thermal ellipsoids and hydrogen atoms and lattice PhMe omitted for clarity. The Yb-*o*-F contacts are indicated by dashed bonds. (* denotes symmetry generated atom)

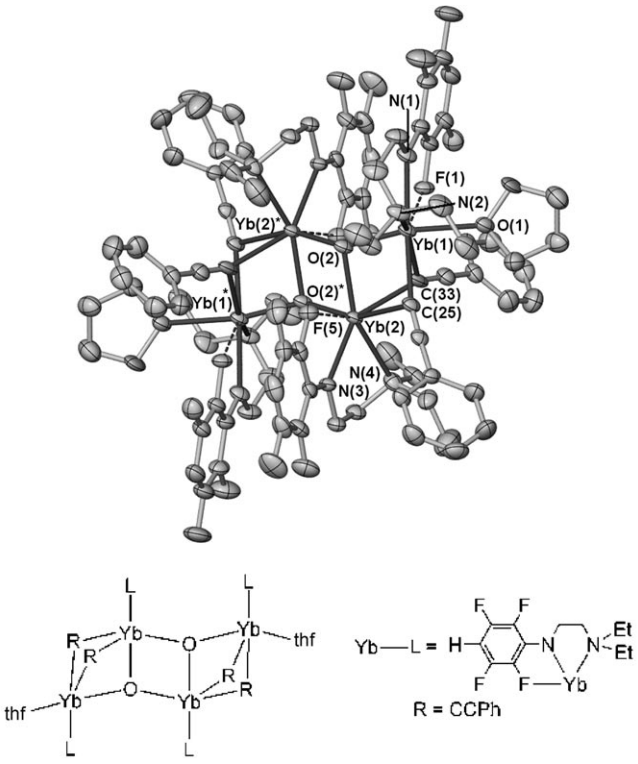

Figure 5. Molecular structure of $[Yb_4(O)_2(L)_4(CCPh)_4(thf)_2]$·THF (**9a**·THF), as shown with 50% thermal ellipsoids along with a schematic representation. Hydrogen atoms and the lattice THF molecule have been omitted for clarity.

On the other hand, Yb(2) is seven coordinate and has a pentagonal bipyramidal geometry with N(5), N(6), F(14), F-(14*) and F(9) being approximately planar and F(13) and F(15) apical (*trans* angle **8a** 162.2(1), **8b**·4PhMe 162.7(1)°). Analysis of the bond lengths (Table 2) shows shorter (ca. 0.15 Å) Yb–N and Yb–F(Ar) bonds by comparison with the ytterbium(II) complex **7a**, as expected on the basis of the respective ionic radii.[36] The Yb–F(fluoride) distances range from 2.148(3) to 2.191(3) Å,and the average distance to Yb(2) is marginally shorter than to Yb(1) consistent with the higher coordination number of the latter. The Yb–F distances in **8a** and **8b** are comparable to those of known ytterbium(III) fluoride clusters with μ_2-F moieties, for example, in eight coordinate $[Yb_4(CpMe)_8(\mu\text{-}F)_4]$ (av 2.154 Å) or $[Yb_3(Cp)_6(\mu\text{-}F)_3]$ (av 2.156 Å).[41]

The reaction pathway leading from the ytterbium(II) compounds $[Yb(L)_2(solv)_n]$, to the fluoride-bridged clusters **8a** and **8b** evidently involves C–F activation and fluorine atom abstraction from the *N*,*N*-dialkyl-*N*′-2,3,5,6-tetrafluorophenylethane-1,2-diaminate ligands (rather than from Hg-$(C_6F_5)_2$ in redox transmetalation/ligand exchange syntheses—see below). Although fluorine atom abstraction has been observed in both lanthanoid(II) and lanthanoid(III) systems (see above), it has been proposed for low-valent lanthanoids that such reactions proceed by single-electron transfer (SET) generating Ln^{III}–F and an organic radical (Scheme 4), which can abstract a H atom from THF.[25,26] GC/MS analyses of hydrolysed reaction mixtures after conversion of **4a** or **4b** in C_6D_6 to **8a** or **8b** showed evidence of defluorination of the ligand. The data for **4a**→**8a** were complex with more than ten components observed in the GC trace, the majority of which appeared to be lower molecular weight compounds, presumably degradation products of LH.

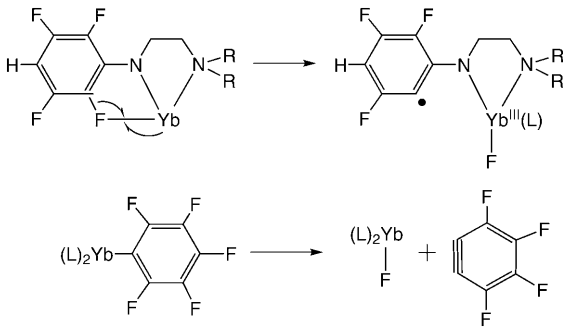

Scheme 4. Possible C–F activation pathways involving SET from Yb^{II} (upper) or F^- transfer and benzyne formation at Yb^{III} (lower).

At longer retention times, three major fractions were observed, containing LH (**1a** *m*/*z* 264), L*H (**1a**−F $C_6F_3H_2N(H)CH_2CH_2Et_2$, *m*/*z* 246) and L**H (**1a**−2F $C_6F_2H_3N(H)CH_2CH_2Et_2$, *m*/*z* 228). The trace for **4b**→**8b** was much simpler and showed only two major fractions (in approximately 20:1 ratio) comprising LH (**1b**, *m*/*z* 236) and L*H (**1b**−F $C_6F_3H_2N(H)CH_2CH_2Me_2$, *m*/*z* 218) respectively. The origin of L*H is presumably from the radical reaction intermediate (Scheme 4, upper). However, the observation of the doubly defluorinated ligand L**H clearly shows that more than one fluorine can be extracted. Furthermore, some of the shorter retention time components of the GC trace resulting from **4a**→**8a** can be assigned to species with an even lower F content, for example, *m*/*z* 207 $C_{12}H_{16}N_2F^+$ ($LH-3F]^+$), plausibly derived from isomers of a monofluorinated ligand. Given the presence of L*H (and L**H) in the reaction solution after hydrolysis, it is notable that no L* was detected in any of the products. Hydrolysis of a bulk sample of **8a** showed LH as the sole significant product. Doubly and triply defluorinated ligands may no longer have *o*-F atoms to enable tridentate coordination to ytterbium and even in the case of L*, putative Yb−*o*-F binding may be weakened, since it has been shown that for [Ce(C_5H_2-*t*Bu_3-1,2,4)$_2$R], Ce-*o*−F bonding is weakened in the series R = C_6F_5 > *m*-HC_6F_4 > *o*-HC_6F_4.[5]

The data described above clearly establishes that **8a** or **8b** are derived from **4a** or **4b** and that the fluoride source is the *N*,*N*-dialkyl-*N*′-2,3,5,6-tetrafluorophenylethane-1,2-diaminate ligands. However, the formation of **8a** or **8b** by the redox transmetalation/ligand exchange method raises the possibility of a contribution from a second C−F activation process. These reactions are also known to give fluoride-containing products through decomposition of intermediate lanthanoid(III) [Ln(L)$_2C_6F_5$] species (L = OAr or ArNCNAr; Scheme 4, lower).[23–24] Whilst initial formation of **4a** or **4b** from Yb/Hg(C_6F_5)$_2$/LH reactions has been shown (see above), involvement of such a reaction path is still plausible. In an attempt to reduce the possible sources of fluoride, we performed the redox transmetalation/ligand exchange reaction of Yb, Hg(C≡CPh)$_2$ and **1a** in THF. This reaction initially gave a dark-brown-yellow solution, but we were unable to isolate a crystalline product. However, after several weeks, pale yellow crystals formed that were shown to be an oxidation product, namely, [Yb_4(L)$_4$(μ-C≡CPh)$_4$(μ$_3$-O)$_2$-(thf)$_2$]·THF (**9a**·THF) by X-ray crystallography. This complex has presumably resulted from accidental exposure to air and we were only able to prepare a bulk sample in moderate yield by deliberate addition of dry air to the reaction solution (Scheme 5).

The presence of the C≡CPh moiety was confirmed by observation of a *ν*(C≡C) frequency (2061 cm^{-1}) in the IR spectrum and ^{19}F NMR resonances were observed at $\delta = -134.3$ and −153.1 ppm, which are near the range observed for paramagnetic [Ln(SC_6F_6)$_3$(solv)$_x$] complexes, although different from those of observed during the decomposition of **4a** or **4b** (see above). Elemental analyses for the dried bulk material were consistent with the structural formula, assuming loss of the lattice THF molecule. The structure of the product (Figure 5) displays a four-rung ladder with the outer rings linked by two μ-C≡CPh and an O bridge, whilst the central rings have Yb_2(μ-O)$_2$ connectivity. As with the complexes described above, the amido ligands are bound to ytterbium in a tridentate (N,N′,F) mode with Yb−N and Yb−F distances (Table 3) comparable with those of **8a** and **8b**.

$$4Yb + 4Hg(CCPh)_2 + 4HL \xrightarrow[-4Hg,\ -4HCCPh]{THF,\ [O_2]} [Yb_4(O)_2(L)_4(CCPh)_4(thf)_2]$$

Scheme 5. Synthesis of **9a** resulting from an attempted redox transmetalation/ligand exchange reaction.

Table 3. Selected bond lengths [Å] in [$Yb_4(O)_2(L)_4(CCPh)_4(thf)_2$]·THF (**9a**·THF; L = *p*-$HC_6F_4N(CH_2)_2NEt_2$).

Yb(1)−N(1)	2.315(6)	Yb(2)−N(3)	2.335(6)
Yb(1)−N(2)	2.558(7)	Yb(2)−N(4)	2.583(7)
Yb(1)−F(1)	2.526(5)	Yb(2)−F(5)	2.527(5)
Yb(1)−C(25)	2.469(8)	Yb(2)−C(25)	2.603(7)
Yb(1)−C(33)	2.469(10)	Yb(2)−C(33)	2.451(9)
Yb(1)−O(2)	2.067(5)	Yb(2)−O(2)	2.253(5)
Yb(1)−O(1)	2.337(5)	Yb(2)−O(2)*[a]	2.101(5)

[a] Symmetry operator *: $-x, -y+1, -z$.

Each ytterbium atom is seven coordinate, bound to an amido ligand, two bridging phenylacetylides, a μ$_3$-oxide and a THF ligand (Yb(1)) or two μ$_3$-oxides (Yb(2)). The Yb−C distances of the bridging phenylacetylide fragments, apart from one outlier (Table 3), are generally consistent with an ytterbium(III) oxidation state, being about 0.12 Å shorter than for the seven coordinate ytterbium(II) complex [{YbI(μ-C≡CPh)(dme)$_2$}$_2$] (av Yb−C 2.593 Å)[42a]—see also mixed valent [$Yb^{III}(Cp^*)_2$(μ-C≡CPh)$_2Yb^{II}$(μ-C≡CPh)$_2Yb^{III}(Cp^*)_2$] (av 2.528 Å to Yb^{II} and 2.401 Å to Yb^{III}[42b]). The presence of residual C≡CPh moieties in the "oxidised" product showed that the ligand exchange reaction of the intermediate {Yb(C≡CPh)$_2$} species with LH was incomplete. This contrasts the high yield of **4a** when Hg(C_6F_5)$_2$ was used as the mercurial (see above).

Conclusion

This study has shown that divalent ytterbium(II) complexes with tridentate (N,N′,F) *N*,*N*-dialkyl-*N*′-2,3,5,6-tetrafluorophenylethane-1,2-diaminate(1−) ligands (L) thermally decompose to heteroleptic ytterbium(III) fluoride species. The ytterbium(II) species [Yb(L)$_2$(solv)$_n$] (solv = thf, dme) can be readily synthesised by ligand exchange, metathesis or redox transmetalation/ligand exchange reactions, but are isolated only at low temperature. The subsequent formation of the fluoride cluster [Yb_4(L)$_6F_6$] is believed to result from fluorine atom abstraction from the polyfluorophenylamido ligands. In this context, the binding of the *N*,*N*-dialkyl-*N*′-2,3,5,6-tetrafluorophenylethane-1,2-diaminate(1−) ligands to ytterbium (in either the II or III oxidation state), is exclu-

sively tridentate through the amido and amine nitrogen atoms as well as one of the *ortho* fluorine atoms. The Yb–F interaction is strong, as indicated by the shorter metal–donor bond length than to the more classical dialkyl amine donor group. Furthermore, the sodium and potassium complexes $[Na(L)_2Na(tmeda)]$ and $[K_2(L)_2(tmeda)_2]$, prepared by ligand exchange, also show *o*-F–M coordination, suggesting that tridentate N,N′,F coordination may be the dominant mode for these ligands with electropositive elements. In the case of low-valent Yb^{II}, C–F bond activation through Yb-*o*-F-C(Ar) coordination is a precursor to metal–fluoride formation.

Experimental Section

General: The compounds described herein were prepared and handled by using conventional air-sensitive techniques. IR spectra for **1a/1b** were recorded as Nujol and HCB mulls on KBr plates with a Perkin Elmer 180 spectrophotometer, whilst spectra for metal complexes were recorded as Nujol mulls on NaCl plates with a Perkin Elmer 1600 FTIR spectrophotometer. Multinuclear NMR spectra were recorded by using a Bruker DPX 300 spectrometer. Chemical shifts were referenced to the residual ^1H resonances of the deuterated solvents (^1H) or external CCl_3F (^{19}F) or $[Yb(C_5Me_5)_2]$ (0.15 M) in THF/C_6D_6 (^{171}Yb). Melting points were determined in sealed glass capillaries under nitrogen and are uncalibrated. Microanalyses were determined by the Australian Microanalytical Service (**1a/1b**) or the Campbell Microanalytical Service, University of Otago (New Zealand). GC/MS data were obtained with a Agilent 6890 series GC fitted with a 5% phenylmethylsiloxane capillary column (Agilent 19091S-433HP-5 MS) and interfaced to a Agilent 5987 network mass selective detector. *N,N*-Diethylethane-1,2-diamine, *N,N*-dimethylethane-1,2-diamine, $NaN(SiMe_3)_2$ (1 M solution in THF) and $KN(SiMe_3)_2$ (0.5 M solution in toluene) were from Aldrich. Pentafluorobenzene from Bristol Organics was dried over sieves (4 Å). $Hg(C_6F_5)_2$,[43a] $Hg(C{\equiv}CPh)_2$,[43b] YbI_2 (0.02 M solution in THF)[43c] and $[Yb\{N(SiMe_3)_2\}_2(thf)_2]$),[32b] were prepared by literature methods.

Synthesis of *p*-$HC_6F_4NHC_2H_4NEt_2$ (1a): Pentafluorobenzene (13.3 g, 79 mmol) and *N,N*-diethylethane-1,2-diamine (18.2 g, 157 mmol) in dry ethanol (15 mL) were heated to reflux under nitrogen for 12 h. Evaporating the solution under vacuum, gave an orange gel The gel was treated with diethyl ether/water and was extracted four times with ether. The combined organic extracts were dried over $MgSO_4$ and then evaporated under vacuum leaving a high boiling point liquid. Two distillations under vacuum, gave pure **1a** (8.4 g, 40%). B.p. 54–56 °C (5×10^{-3} mmHg); IR: $\tilde{\nu}$ = 3335 (m, br), 3097 (w), 2970 (s), 2938 (m), 2896 (m), 2876 (m), 2818 (m), 1648 (vs), 1605 (m), 1521 (vs), 1507 (sh), 1482 (s), 1471 (s), 1455 (s), 1401 (w), 1382 (m), 1371 (m), 1346 (m), 1297 (m), 1272 (w), 1257 (m), 1240 (m), 1201 (m), 1159 (s), 1143 (s), 1126 (m), 1065 (s), 1019 (w), 948 (m), 922 (w), 908 (m), 817 (w), 791 (m), 740 (w), 709 (m), 663 (w), 566 (w), 466 (w), 432 cm^{-1} (w); ^1H NMR ($CDCl_3$, 298 K): δ = 1.02 (t, ^3J(H,H) = 7.12 Hz, 6H; CH_3), 2.52 (q, ^3J(H,H) = 7.12 Hz, 4H; CH_2, NEt_2), 2.65 (t, ^3J(H,H) = 5.68 Hz, 2H; CH_2, CH_2NEt_2), 3.40 (m, 2H; CH_2NAr), 4.83 (brs, 1H; NH), 6.34 ppm (tt, ^3J(H,F) = 10.10 Hz, ^4J(H,F) = 7.06 Hz, 1H; HC_6F_4); ^{19}F NMR ($CDCl_3$, 298 K): δ = −142.3 (m, 2F; F3,5), −160.8 (m, 2F; F2,6); elemental analysis calcd (%) for $C_{12}H_{16}F_4N_2$ (264.26): C 54.54, H 6.10, N 10.60; found: C 54.8, H 6.3, N 10.7.

Synthesis of *p*-$HC_6F_4NHC_2H_4NMe_2$ (1b): By using a similar procedure, **1b** (12.6 g, 41%) was obtained from pentafluorobenzene (21.8 g, 130 mmol) and *N,N*-dimethylethane-1,2-diamine (22.0 g, 250 mmol) in dry ethanol (20 mL). B.p. 53 °C (5×10^{-2} mmHg); IR: $\tilde{\nu}$ = 3357 (m, br), 3094 (w), 2977 (m), 2927 (s), 2889 (m), 2861 (m), 2813 (s), 2774 (s), 1649 (vs), 1608 (m), 1523 (vs), 1511 (sh), 1481 (s), 1459 (vs), 1401 (m), 1376 (w), 1347 (m), 1328 (w), 1282 (m), 1261 (m), 1243 (s), 1182 (m), 1160 (vs), 1140 (vs), 1098 (m), 1073 (s), 1056 (s), 1040 (s), 968 (s), 925 (vs), 873 (w), 788 (m), 710 (m), 662 (w), 565 (w), 526 (w), 464 cm^{-1} (w); ^1H NMR ($CDCl_3$, 298 K): δ = 2.26 (brs, 6H; CH_3), 2.51 (t, ^3J(H,H) = 5.78 Hz, 2H; CH_2NMe_2), 3.41 (m, 2H; CH_2NAr), 4.64 (brs, 1H; NH), 6.35 ppm (tt, ^3J(H,F) = 10.08 Hz, ^4J(H,F) = 7.04 Hz, 1H; HC_6F_4); ^{19}F NMR ($CDCl_3$, 282.4 MHz): δ = −142.3 (m, 2F; F3,5), −161.0 ppm (m, 2F; F2,6); elemental analysis calcd (%) for $C_{10}H_{12}F_4N_2$ (236.21): C 50.85, H 5.12, F 32.17, N 11.86; found: C 51.0, H 5.1, F 32.0, N 12.0.

[Na(*p*-$HC_6F_4NC_2H_4NEt_2$)] (2a): A solution of $NaN(SiMe_3)_2$ in THF (1 M, 6.0 mL, 6.0 mmol) was added with stirring to a solution of **1a** (1.59 g, 6.0 mmol) in THF (20 mL). The mixture was stirred for 0.5 h and the solvent was then removed under vacuum. The residue was washed with toluene (10 mL × 2) and dried under vacuum for 1 h to leave **2a** as an off-white powder (1.58 g, 92%). M.p. 158–162 °C. IR: $\tilde{\nu}$ = 1641 (s), 1557 (s), 1452 (s), 1385 (m), 1344 (s), 1291 (s), 1256 (w), 1236 (m), 1188 (w), 1175 (w), 1145 (m), 1066 (m), 1050 (w), 1002 (m), 924 (s), 855 (m), 799 (w), 748 (w), 733 (m), 716 (w), 688 cm^{-1} (w); ^1H NMR (C_4D_8O, 303 K): δ = 0.78 (t, ^3J = 7.17 Hz, 6H; CH_3), 2.35 (brs, 4H; CH_2, NEt_2), 2.51 (brs, 2H; CH_2NEt_2), 4.02 (brs, 2H; CH_2NAr), 5.61 ppm (brs, 1H; HC_6F_4); ^{19}F NMR (C_4D_8O, 303 K): δ = −147.8 (brs, 2F; F3,5), −173.1 ppm (brs, 2F; F2,6); elemental analysis calcd (%) for $C_{12}H_{15}F_4N_2Na$ (286.24): C 50.35, H 5.28, N 9.79; found: C 50.41, H 5.35, N 9.10.

[K(*p*-$HC_6F_4NC_2H_4NEt_2$)] (3a): By using a similar procedure, a solution of $KN(SiMe_3)_2$ in PhMe (0.5 M, 12 mL, 6.0 mmol) and **1a** (1.59 g, 6.0 mmol) in THF (20 mL) gave **3a** as an off-white powder (1.72 g, 95%). M.p. 192–196 °C; IR: $\tilde{\nu}$ = 1644 (m), 1550 (m), 1504 (w), 1353 (w), 1284 (w), 1268 (w), 1229 (w), 1192 (w), 1169 (w), 1138 (m), 1086 (w), 1058 (w), 1024 (m), 924 (m), 890 (w), 863 (w), 706 (w), 688 (w), 668 cm^{-1} (w); ^1H NMR (C_4D_8O, 303 K): δ = 0.86 (t, ^3J = 7.18 Hz, 6H; CH_3), 2.45 (q, ^3J = 7.14 Hz, 4H; CH_2, NEt_2), 2.51 (t, ^3J = 5.86 Hz, 2H; CH_2NEt_2), 3.75 (m, 2H; CH_2NAr), 5.30 ppm (m, 1H; HC_6F_4); ^{19}F NMR (C_4D_8O, 303 K): δ = −148.2 (brs, 2F; F3,5), −170.0 ppm (brs, 2F; F2,6); ^{19}F NMR (C_4D_8O, 203 K): δ = −147.7 (s, 1F, F3 or F5), −151.4 (s, 1F, F3 or F5), −168.7 (s, 1F, F2 or F6), −173.3 ppm (s, 1F, F2 or F6); elemental analysis calcd (%) for $C_{12}H_{15}F_4N_2K$ (302.35): C 47.67, H 5.00, N 9.27; found: C 47.11, H 5.35, N 9.10.

[Yb(*p*-$HC_6F_4NC_2H_4NEt_2$)$_2$(thf)$_2$] (4a)

Method A: A solution of $[Yb\{N(SiMe_3)_2\}_2(thf)_2]$ (1.28 g, 2.0 mmol) in hexane (20 mL) was added to a solution of **1a** (1.06 g, 4.0 mmol) in THF (3.0 mL). The mixture was stored at −30 °C overnight during which time deep orange crystals of **4a** deposited, which were collected by decantation and dried under vacuum (1.20 g, 71%). M.p. 98–102 °C; IR: $\tilde{\nu}$ = 1640 (s), 1558 (w), 1353 (m), 1301 (m), 1245 (w), 1147 (s), 1056 (m), 943 (s), 900 (w), 877 (w), 738 (w), 726 cm^{-1} (w); ^1H NMR (C_6D_6, 303 K): δ = 0.68 (brt, 12H; CH_3), 1.30 (brs, 8H; OC_4H_8), 2.39–2.44 (brm, 12H; CH_2, NEt_2 + CH_2NEt_2), 3.47 (brs, 8H; OC_4H_8), 3.81 (brs, 4H; CH_2NAr), 5.72 ppm (brm, 2H; HC_6F_4); ^{19}F NMR (C_6D_6, 303 K): δ = −145.3 (brs, 4F; F3,5), −164.8 ppm (brs, 4F; F2,6); ^{19}F NMR (C_7H_8, 203 K): δ = −141.6 (s, 2F; F3 or F5), −148.2 (s, 2F; F3 or F5), −159.8 (brs, 2F; F2 or F6), −167.1 ppm (s, 2F; F2 or F6); ^{171}Yb NMR (C_7D_8, 303 K): δ = 490 (brs); (203 K), 405 ppm (brs); ^{171}Yb NMR (C_6D_6/THF, v/v, 2:1, 303 K): δ = 398 ppm; elemental analysis calcd (%) for $C_{28}H_{38}F_8N_4OYb$ (loss of one THF, 771.65): C 43.58, H 4.96, N 7.26; found: C 42.77, H 5.09, N 7.30.

Method B: Yb metal powder (0.69 g, 4.0 mmol), $Hg(C_6F_5)_2$ (1.07 g, 2.0 mmol), and **1a** (1.06 g, 4.0 mmol) in THF (30 mL) were stirred at room temperature for 48 h. The reaction mixture was filtered, followed by evaporation of THF under vacuum to 3 mL. Hexane (20 mL) was added and the mixture was stored at −30 °C overnight depositing deep orange crystals of **4a** (yield: 0.71 g, 46%). The ^1H NMR and ^{19}F NMR spectra were identical with those given above.

Method C: A solution of **3a** (0.60 g, 2.0 mmol) in THF (20 mL) was added to a solution of YbI_2 in THF (0.02 M, 50 mL, 1.0 mmol). The mixture was stirred for 2 h, followed by evaporation of THF under vacuum and addition of toluene (30 mL). The resulting precipitate was filtered off and the volume of the filtrate was reduced to 4 mL under vacuum. Hexane (20 mL) was added and the mixture was stored at −30 °C overnight depositing deep orange crystalline **4a** (1.00 g, 64%). The ^1H NMR and ^{19}F NMR spectra were identical with those given above.

[Yb(p-HC$_6$F$_4$NC$_2$H$_4$NMe$_2$)$_2$(thf)$_2$] (4b)

Method A: The preparation was effected as in method A for **4a** from [Yb{N(SiMe$_3$)$_2$}$_2$(thf)$_2$] (1.28 g, 2.0 mmol) and **1b** (0.94 g, 4.0 mmol) and afforded deep orange crystalline **4b** (yield: 1.00 g, 73%). M.p. 126°C (decomp); IR: $\tilde{\nu}$=1645 (m), 1558 (w), 1456 (m), 1298 (w), 1142 (m), 1060 (w), 958 (w), 926 (m), 789 cm^{-1} (w). ^{1}H NMR (C$_6$D$_6$, 300.132 MHz): δ= 1.23 (brs, 8H; OC$_4$H$_8$), 1.85 (s, 12H; NCH$_3$), 2.13 (brs, 4H; CH$_2$NR$_2$), 3.43 (brs, 8H; OC$_4$H$_8$), 3.78 (brs, 4H; CH$_2$NAr), 5.73 ppm (brs, 2H; HC$_6$F$_4$); ^{19}F NMR (C$_6$D$_6$, 303 K): δ=−145.1 (brs, 4F; F3,5), −165.0 ppm (brs, 4F; F2,6); elemental analysis calcd (%) for C$_{24}$H$_{30}$F$_8$N$_4$OYb (loss of one THF, 715.55): C 40.28, H 4.23, N 7.83; found: C 40.58, H 4.71, N 7.55.

Method B: The reaction was effected as in method B for **4a** using Yb metal powder (0.69 g, 4.0 mmol), Hg(C$_6$F$_5$)$_2$ (1.07 g, 2.0 mmol), and **1b** (0.94 g, 4.0 mmol) and afforded deep orange crystalline **4b** (yield: 0.73 g, 61%). The ^{1}H NMR and ^{19}F NMR spectra were identical with those given above.

[Na$_2$(p-HC$_6$F$_4$NC$_2$H$_4$NEt$_2$)$_2$(tmeda)] (5a): TMEDA (2.09 g, 18 mmol) and PhMe (5 mL) were added to **2a** (0.86 g, 3.0 mmol) and the resulting slurry was warmed to leave a clear faintly purple solution. After storing at −30°C for one week, colourless crystals of **5a** were collected by filtration and dried under vacuum (0.66 g, 70%). M.p. 152–156°C; IR: $\tilde{\nu}$= 1637 (m), 1556 (w), 1342 (m), 1299 (m), 1264 (w), 1239 (w), 1186 (w), 1141 (m), 1122 (w), 1064 (m), 1006 (w), 932 (s), 855 (w), 788 (w), 733 (m), 690 cm^{-1} (w); ^{1}H NMR (C$_4$D$_8$O, 303 K): δ=0.66 (brs, 12H; CH$_3$), 1.65 (s, 4H; NCH$_2$, tmeda), 1.82 (s, 12H; NCH$_3$, tmeda), 2.19 (brs, 8H; CH$_2$, NEt$_2$), 2.58 (brs, 4H; CH$_2$NEt$_2$), 3.84 (brs, 4H; CH$_2$NAr), 5.70 ppm (brs, 2H; HC$_6$F$_4$); ^{19}F NMR (C$_4$D$_8$O, 303 K): δ=−145.7 (brs, 4F; F3,5), −171.0 ppm (brs, 4F; F2,6); elemental analysis calcd (%) for C$_{27}$H$_{38}$F$_8$N$_5$Na$_2$ (loss of 0.5 tmeda, 630.59): C 51.43, H 6.07, N 11.11; found: C 50.51, H 6.37, N 11.42.

[K$_2$(p-HC$_6$F$_4$NC$_2$H$_4$NEt$_2$)$_2$(tmeda)$_2$] (6a): Using a similar procedure, TMEDA (2.09 g, 18 mmol) and **3a** (0.91 g, 3.0 mmol) in THF (5.0 mL) gave colourless crystals of **6a** (0.77 g, 61%). M.p. 177–181°C; IR: $\tilde{\nu}$= 1648 (m), 1550 (w), 1524 (w), 1294 (w), 1143 (m), 1034 (w), 925 (w), 782 (w), 688 cm^{-1} (w); ^{1}H NMR (C$_4$D$_8$O, 303 K): 1.03 (t, ^3J=7.50 Hz, 12H; CH$_3$), 2.18 (s, 24H; NCH$_3$, tmeda), 2.33 (s, 8H; NCH$_2$, tmeda), 2.58–2.63 (m, 12H; CH$_2$, NEt$_2$+CH$_2$NEt$_2$), 3.70 (m, 4H; CH$_2$NAr), 5.22 ppm (brs, 2H; HC$_6$F$_4$); ^{19}F NMR (C$_4$D$_8$O, 282.4 MHz): δ=−148.7 (brs, 4F; F3,5), −169.6 ppm (brs, 4F; F2,6); elemental analysis calcd (%) for C$_{33}$H$_{54}$F$_8$K$_2$N$_7$ (loss of 0.5 tmeda, 779.01): C 50.88, H 6.99, N 12.59; found: C 50.42, H 6.52, N 12.83.

[Yb(p-HC$_6$F$_4$NC$_2$H$_4$NEt$_2$)$_2$(dme)] (7a): DME (15 mL) was added to **4a** (0.84 g, 1.0 mmol), and the mixture was warmed up gently and kept at 40°C till all solid was dissolved. The solution was stored at −30°C for three days, during which time, deep orange prisms of **7a** were deposited and collected by filtration (yield: 0.64 g, 81%). M.p. 152°C (decomp); IR: $\tilde{\nu}$=1645 (s), 1558 (m), 1500 (m), 1456 (s), 1351 (m), 1298 (m), 1269 (w), 1244 (w), 1208 (w), 1148 (s), 1061 (s), 1036 (w), 945 (s), 904 (w), 862 (m), 788 (w), 728 (m), 692 cm^{-1} (w); ^{1}H NMR (C$_6$D$_6$, 303 K): δ=0.78 (brs, 12H; NCH$_3$), 2.50 (brs, 12H; NEt$_2$+CH$_2$NEt$_2$), 2.86 (brs, 6H; OCH$_3$), 2.96 (brs, 4H; OCH$_2$), 3.80 (brs, 4H; CH$_2$NAr), 5.68 ppm (brs, 2H; HC$_6$F$_4$); ^{19}F NMR (C$_6$D$_6$, 303 K): δ=−142.9 (brs, 2F; F3 or F5), −148.8 (brs, 2F; F3 or F5), −162.2 (brs, 2F; F2 or F6), −166.6 ppm (brs, 2F; F2 or F6); ^{19}F NMR (C$_6$D$_6$, 333 K): δ=−145.8 (brs, 4F; F3,5), −164.3 ppm (brs, 4F; F-2,6); ^{171}Yb NMR (C$_6$D$_6$, 303 K): δ=389 ppm (brs); elemental analysis calcd (%) for C$_{28}$H$_{40}$F$_8$N$_4$O$_2$Yb (789.67): C 42.59, H 5.11, N 7.09; found: C 42.30, H 5.28, N 7.16

[Yb$_4$F$_6$(p-HC$_6$F$_4$NC$_2$H$_4$NEt$_2$)$_6$] (8a)

Method A: Yb metal powder (1.04 g, 6.0 mmol), Hg(C$_6$F$_5$)$_2$ (1.60 g, 3.0 mmol), and **1a** (1.59 g, 6.0 mmol) in THF (40 mL) were stirred at room temperature for 48 h. The reaction mixture was filtered and the solvent was removed under vacuum giving a light orange solid. The material was dissolved in toluene (15 mL), stored at ambient temperature for four weeks and yielded crystalline, light yellow **8a** (1.01 g, 56%). M.p. 236–240°C; IR: $\tilde{\nu}$=1640 (s), 1559 (m), 1353 (m), 1301 (m), 1148 (s), 1056 (m), 943 (m), 905 (w), 878 cm^{-1} (w); elemental analysis calcd (%) for C$_{72}$H$_{90}$F$_{30}$N$_{12}$Yb$_4$ (2385.68): C 36.25, H 3.80, N 7.05; found: C 37.26, H 4.17, N 6.90.

Method B: An NMR tube was charged with **4a** (42 mg, 0.050 mmol) and toluene (0.7 mL). The mixture was shaken until the solid dissolved. The solution was then stored at ambient temperature for two weeks, during which time, light yellow crystals of **8a** precipitated and were collected by decanting the solution (22 mg, 75%). The identity of **8a** was confirmed by crystallography (unit cell data, a=12.846, b=13.740, c=14.176 Å, α= 110.503, β=91.705, γ=116.446°, V=2045.7 Å^3).

Method C: In a similar procedure as to method B **4a** (42 mg, 0.050 mmol) dissolved in C$_6$D$_6$ (0.7 mL) gave light yellow crystals of

Table 4. Crystal and refinement data

	5a	**6a**	**7a**	**8a**	**8a**·C$_6$D$_6$	**8b**·4PhMe	**8b**·2THF	**9a**·THF
formula	C$_{30}$H$_{46}$F$_8$N$_6$Na$_2$	C$_{36}$H$_{62}$F$_8$K$_2$N$_8$	C$_{28}$H$_{40}$F$_8$O$_2$Yb	C$_{72}$H$_{90}$F$_{30}$N$_{12}$Yb$_4$	C$_{78}$H$_{90}$D$_6$F$_{30}$N$_{12}$Yb$_4$	C$_{88}$H$_{98}$F$_{30}$N$_{12}$Yb$_4$	C$_{68}$H$_{82}$F$_{30}$N$_{12}$O$_2$Yb$_4$	C$_{92}$H$_{104}$F$_{16}$N$_8$O$_5$Yb$_4$
M_r	688.71	837.14	789.68	2385.72	2469.86	2585.94	2361.62	2397.99
crystal system	monoclinic	triclinic	monoclinic	triclinic	monoclinic	triclinic	triclinic	monoclinic
space group	$C2/c$	$P\bar{1}$	$P2_1/n$	$P\bar{1}$	$C2/c$	$P\bar{1}$	$P\bar{1}$	$P2_1/n$
a [Å]	16.6428(3)	10.3338(4)	12.3616(2)	12.8010(3)	25.4776(7)	12.4627(3)	11.7179(3)	15.6045(4)
b [Å]	14.1155(4)	10.9026(4)	17.8526(3)	13.6775(3)	12.9552(4)	13.2767(3)	13.7708(4)	15.3027(4)
c [Å]	16.2581(4)	11.5087(5)	13.9943(2)	14.1239(5)	28.7497(8)	16.1705(4)	14.3926(4)	18.7041(5)
α [°]	90	85.214(2)	90	110.462(1)	90	87.763(1)	113.182(2)	90
β [°]	115.75(2)	65.010(2)	90.223(1)	91.795(1)	114.199(2)	67.482(1)	95.523(1)	94.635(1)
γ [°]	90	70.277(2)	90	116.416(1)	90	72.820(1)	109.630(1)	90
V [Å^3]	3439.67(14)	1103.64(8)	3088.33(8)	2022.85(10)	8655.5(5)	2353.02(10)	1939.58(10)	4451.8(2)
Z	4	1	4	1	4	1	1	2
ρ_{calcd} [g cm^{-3}]	1.330	1.260	1.698	1.958	1.895	1.825	2.022	1.789
μ [mm^{-1}]	0.132	0.283	3.109	4.700	4.397	4.048	4.902	4.253
$2\Theta_{max}$	55.0	55.0	50.0	55.0	50.0	55.0	55.0	55.0
N_t	13362	19591	55357	26436	20425	22742	23029	143633
N (R_{int})	3919 (0.065)	4926 (0.034)	5419 (0.029)	9245 (0.045)	7515 (0.082)	10527 (0.059)	8849 (0.055)	10288 (0.048)
N [$I>2\sigma(I)$]	2956	4576	4567	7440	4470	7896	6296	8671
$R1$/w$R2$[a]	0.056/0.157	0.049/0.125	0.024/0.059	0.034/0.063	0.059/0.130	0.047/0.108	0.040/0.066	0.049/0.103
$R1$/w$R2$[b]	0.080/0.173	0.053/0.128	0.031/0.065	0.049/0.067	0.118/0.156	0.070/0.119	0.076/0.075	0.065/0.116
GOF	1.037	1.103	1.062	1.062	0.996	1.007	1.015	1.189
max/min Δe [e Å^{-3}]	0.571/−0.497	1.045/−0.424	2.35/−0.77	1.190/−1.894	2.457/−2.227	2.504/−2.489	1.216/−1.332	3.963/−3.145[c]

[a] [$I>2\sigma(I)$]. [b] All data. [c] Highest residual peak 3.963 e Å^{-3} is located 0.793 Å from Yb(1).

8a·C_6D_6 (22 mg, 70%). The compound was identified by X-ray crystallography (see Table 4).

[Yb_4F_6(*p*-$HC_6F_4NC_2H_4NMe_2$)$_6$] (8b)

Method A: The preparation was effected as in **8a** above from Yb metal powder (1.04 g, 6.0 mmol), $Hg(C_6F_5)_2$ (1.60 g, 3.0 mmol), and **1b** (1.42 g, 6.0 mmol) to afford light yellow crystals of **8b**·4PhMe (1.16 g, 67%). M.p. 210°C (decomp); IR: $\tilde{\nu}$ = 1650 (m), 1578 (m), 1353 (m), 1300 (w), 1281 (w), 1141 (s), 1058 (m), 958 (m), 929 (m), 758 (w), 728 (m), 694 cm^{-1} (w). elemental analysis calcd (%) for $C_{60}H_{66}F_{30}N_{12}Yb_4$ (loss of toluene of solvation, 2217.36): C 32.50, H 3.00, N 7.58; found: C 31.92, H 3.16, N 7.27. Crystals of **8b**·2THF were obtained by crystallisation from initial filtered THF solution.

Method B: A flask was charged with **4b** (0.79 g, 1.0 mmol) and toluene (5 mL). The solution was kept at 50°C for 2 h and then stored at ambient temperature for three weeks, during which time, light yellow crystals of **8b**·4PhMe deposited (0.47 g, 82%). The identity of **8b**·4PhMe was confirmed by IR and crystallography (unit cell data, a = 12.443(4), b = 13.267(4), c = 16.144(5) Å, α = 87.74(3), β = 67.54(3), γ = 72.79(3), V = 2344.3(12) $Å^3$). In a parallel experiment performed in an NMR tube, **4b** (39 mg, 0.050 mmol) in toluene/C_7D_8 (1:1, 0.7 mL) was kept at ambient temperature for two weeks. ^{19}F NMR (303 K): δ = 103.1 (br s, 2F), −30.6 (s, 4F), −130.5 (s, 12F; F3,5), −182.3 ppm (s, 12F; F2,6).

Method C: A flask containing **4b** (0.79 g, 1.0 mmol) and perfluorohexane (5 drops) in toluene (5 mL) was kept at 50°C for 2 h and then stored at ambient temperature for three weeks, during which time, light yellow crystalline **8b**·4PhMe deposited (0.31 g, 54%). The identity of **8b**·4PhMe was confirmed by IR and crystallography.

GC/MS analyses of reaction mixtures: Following the procedures above, **4a** or **4b** (ca. 50 mg) was loaded into a NMR tube and dissolved in C_6D_6. These solutions were kept at ambient temperature for two weeks and were monitored by ^{19}F NMR spectroscopy. During this time, yellow crystals of **8a** or **8b** formed. The reactions were quenched by addition of EtOH or MeOH, and the filtered organic fractions analysed by GC/MS. **4a**→**8a** (major fractions only): R_t: 4.65 (m/z 104), 5.33 (m/z 129), 9.00 (m/z 207), 9.24 (m/z 207), 9.97 (m/z 158), 10.29 (m/z 207), 10.62 (m/z 207), 14.43 (m/z 264, $[LH]^+$), 15.21 (m/z 246 $[LH_2-F]^+$), 15.63 min (m/z 228, $[LH_3-2F^+]$). **4b**→**8b** (major fractions only): R_t: 10.04 (m/z 236, $[LH]^+$), 10.68 min (m/z 218, $[LH_2-F]^+$). An isolated sample of **8a** (ca 40 mg) was hydrolysed in PhMe/EtOH and the filtered organic fraction was analysed by GC/MS: R_t: 10.90 min (m/z 264 $[LH]^+$).

[Yb_4(*p*-$HC_6F_4NC_2H_4NEt_2$)$_4$(μ_3-O)$_2$(μ_2-C≡CPh)$_4$(thf)$_2$] (9a): A Schlenk flask was charged with Yb (1.04 g, 6.0 mmol), $Hg(C{\equiv}CPh)_2$ (1.26 g, 3.0 mmol), and **1a** (1.60 g, 6.0 mmol) and THF (40 mL). The mixture was exposed to dry air and then stirred at room temperature for 48 h. The insoluble material was filtered off and the volume of the filtrate was reduced to 10 mL and stored at ambient temperature for two weeks, during which time, light yellow crystals of **9a**·THF deposited (0.58 g, 32%, based on $Hg(C{\equiv}CPh)_2$). M.p. 190°C (decomp); IR: $\tilde{\nu}$ = 2061 (w), 1645 (m), 1573 (w), 1504 (m), 1353 (w), 1303 (w), 1148 (m), 1062 (m), 948 (m), 758 (m), 694 cm^{-1} (w); ^{19}F NMR (C_6D_6, 303 K): δ = −134.3 (br s, 8F, F3,5), −153.1 ppm (br s, 8F, F2,6); elemental analysis calcd (%) for $C_{88}H_{96}F_{16}N_8O_4Yb_4$ (loss of THF of solvation, 2325.89): C 45.44, H 4.16, N 4.82; found: C 45.23, H 4.49, N 4.52. A significant yield of **9a** could not be obtained without the admission of dry air.

X-ray crystallography: Crystalline samples of compounds were mounted in a thin-walled glass capillary (**6a**) or on glass fibres in highly viscous perfluoropoly ether oil (**5a**) or paraffin oil (**7a**, **8a**, **8a**·C_6D_6, **8b**·2THF, **8b**·4PhMe and **9a**·THF). Diffraction data were obtained at −150°C (123 K) by using an Enraf–Nonius Kappa CCD or Bruker X8 APEX II CCD diffractometer ($Mo_{K\alpha}$ radiation, λ = 0.71073 Å). Each data set was empirically corrected for absorption (SORTAV;[44a] SADABS[44b]) then merged (R_{int} as quoted) to N unique reflections. The structures were solved by conventional methods and refined by full-matrix least-squares on all F^2 data using SHELX97,[44c] in conjunction with the X-Seed graphical user interface.[44d] Crystal data and refinement details are given in Table 4. CCDC-707324 (**5a**), 707325 (**6a**), 707326 (**7a**), 707327 (**8a**), 707328 (**8a**·C_6D_6), 707329 (**8b**·2THF) 707330 (**8b**·4PhMe) and 707331 (**9a**·THF) contain the supplementary crystallographic data for this paper. These data can be obtained free of charge from The Cambridge Crystallographic Data Centre via www.ccdc.cam.ac.uk/data_request/cif.

Acknowledgement

Dr D. P. Buxton is gratefully acknowledged for the initial synthesis of the ligands **1a** and **1b**. This work was financially supported by grants from the Australian Research Council.

[1] F. Castillo, T. D. Tilley, *J. Am. Chem. Soc.* **2001**, *123*, 10526–10534.
[2] P. G. Hayes, G. C. Welch, D. J. H. Emslie, C. L. Noack, W. E. Piers, M. Parvez, *Organometallics* **2003**, *22*, 1577–1579.
[3] G. B. Deacon, C. M. Forsyth, *Organometallics* **2003**, *22*, 1349–1352.
[4] L. Maron, E. L. Werkema, L. Perrin, O. Eisenstein, R. A. Andersen, *J. Am. Chem. Soc.* **2005**, *127*, 279–292.
[5] E. L. Werkema, R. A. Andersen, *J. Am. Chem. Soc.* **2008**, *130*, 7153–7165.
[6] D. R. Click, B. L. Scott, J. G. Watkin, *Chem. Commun.* **1999**, 633–634.
[7] H. Memmler, K. Walsh, L. H. Gade, J. W. Lauher, *Inorg. Chem.* **1995**, *34*, 4062–4068.
[8] A. Lara-Sanchez, A. Rodriguez, D. L. Hughes, M. Schormann, M. Bochmann, *J. Organomet. Chem.* **2002**, *663*, 63–69.
[9] K. Norton, T. J. Emge, J. G. Brennan, *Inorg. Chem.* **2007**, *46*, 4060–4066.
[10] J. H. Melman, C. Rohde, T. J. Emge, J. G. Brennan, *Inorg. Chem.* **2002**, *41*, 28–33.
[11] J. H. Melman, T. J. Emge, J. G. Brennan, *Inorg. Chem.* **2001**, *40*, 1078–1081.
[12] a) S. Banerjee, T. J. Emge, J. G. Brennan, *Inorg. Chem.* **2004**, *43*, 6307–6312; b) M. Roanelli, A. Kumar, T. J. Emge, R. E. Riman, J. G. Brennan, *Angew. Chem.* **2008**, *120*, 6136–6140; *Angew. Chem. Int. Ed.* **2008**, *47*, 6049–6051.
[13] X. Li, J. Baldamus, M. N. Nishura, O. Tardif, Z. Hou, *Angew. Chem.* **2006**, *118*, 8364–8368; *Angew. Chem. Int. Ed.* **2006**, *45*, 8184–8188.
[14] M. W. Bouwkamp, P. H. M. Budzelaar, J. Gorcama, I. D. H. Morales, J. de Wolf, A. Meetsma, S. I. Troyanov, J. H. Teuben, B. Hessen, *J. Am. Chem. Soc.* **2005**, *127*, 14208–14222.
[15] W. J. Evans, K. J. Forrestal, M. A. Ansari, J. W. Ziller, *J. Am. Chem. Soc.* **1998**, *120*, 2180–2181.
[16] H. Takemura, S. Nakashima, N. Kori, M. Yasutake, T. Shinmyozu, T. Inazu, *J. Am. Chem. Soc.* **2001**, *123*, 9293–9298.
[17] W. J. Evans, D. G. Giarikos, M. A. Johnston, M. A. Greci, J. W. Ziller, *J. Chem. Soc. Dalton Trans.* **2002**, 520–526.
[18] D. C. Bradley, H. Chudzyriska, M. E. Hammond, M. Hursthouse, M. Motevalli, V. Ruower, *Polyhedron* **1992**, *11*, 375–379.
[19] P. L. Watson, T. H. Tulip, I. Williams, *Inorg. Chem.* **1990**, *29*, 1999–2009.
[20] D. O'Hagan, *Chem. Soc. Rev.* **2008**, *37*, 308–319.
[21] a) J. L. Kiplinger, T. G. Richmond, C. L. Osterberg, *Chem. Rev.* **1994**, *94*, 373–431; b) J. Burdeniuc, B. Jedlicka, R. H. Crabtree, *Chem. Ber.* **1997**, *130*, 145–154; c) H. Dorn, E. F. Murphy, S. A. A. Shah, H. W. Roesky, *J. Fluorine Chem.* **1997**, *86*, 121–125.
[22] C. J. Burns, R. A. Andersen, *J. Chem. Soc. Chem. Commun.* **1989**, 136–137.
[23] G. B. Deacon, G. D. Fallon, C. M. Forsyth, S. C. Harris, P. C. Junk, B. W. Skelton, A. H. White, *Dalton Trans.* **2006**, 802–812.
[24] a) M. L. Cole, G. B. Deacon, P. C. Junk, K. Konstas, *Chem. Commun.* **2005**, 1581–1583; b) M. L. Cole, G. B. Deacon, C. M. Forsyth, P. C. Junk, K. Konstas, J. Wang, *Chem. Eur. J.* **2007**, *13*, 8092–8110; c) M. L. Cole, P. C. Junk, *Chem. Commun.* **2005**, 2695–2697.
[25] G. B. Deacon, A. J. Koplick, W. D. Raverty, D. G. Vince, *J. Organomet. Chem.* **1979**, *182*, 121–141.
[26] a) G. B. Deacon, P. I. MacKinnon, T. D. Tuong, *Aust. J. Chem.* **1983**, *36*, 43–53; b) G. B. Deacon, C. M. Forsyth, J. Sun, *Tetrahedron Lett.* **1994**, *35*, 1095–1098.

[27] a) C. J. Burns, D. J. Berg, R. A. Andersen, *J. Chem. Soc. Chem. Commun.* **1987**, 272–273; b) G. B. Deacon, S. C. Harris, G. Meyer, D. Stellfeldt, D. L. Wilkinson, G. Zelesney, *J. Organomet. Chem.* **1998**, *552*, 165–170; c) G. B. Deacon, G. Meyer, D. Stellfeldt, *Eur. J. Inorg. Chem.* **2000**, 1061–1071.
[28] a) Z. Xie, K. Chui, Q. Yang, T. C. W. Mak, J. Sun, *Organometallics* **1998**, *17*, 3937–3944; b) Z. Xie, Z. Lui, F. Xue, T. C. W. Mak, *J. Organomet. Chem.* **1997**, *539*, 127–130.
[29] H. Schumann, M. R. Keitsch, J. Winterfeld, J. Demschuk, *J. Organomet. Chem.* **1996**, *525*, 279–281.
[30] A. C. Hillier, X. W. Zhang, G. H. Maunder, S. Y. Liu, T. A. Eberspacher, M. V. Metz, R. McDonald, A. Domingos, N. Marques, V. W. Day, A. Sella, J. Takats, *Inorg. Chem.* **2001**, *40*, 5106–5116.
[31] a) D. P. Buxton G. B. Deacon, B. M. Gatehouse, I. L. Grayson, D. St. C. Black, *Aust. J. Chem.* **1988**, *41*, 943–956; b) G. B. Deacon, B. M. Gatehouse, J. Ireland, *Aust. J. Chem.* **1991**, *44*, 1669–1681; c) a preliminary report of the preparation of **1b** without experimental details or characterisation has been given in : D. P. Buxton, G. B. Deacon, A. M. James, S. J. Knowles, T. L. Williams, *Polyhedron* **1989**, *8*, 2943–2945.
[32] a) G. B. Deacon, E. E. Delbridge, B. W. Skelton, A. H. White, *Eur. J. Inorg. Chem.* **1998**, 543–545; b) G. B. Deacon, G. D. Fallon, C. M. Forsyth, H. Schumann, R. Weimann, *Chem. Ber.* **1997**, *130*, 409–415; c) J. R. van den Hende, P. B. Hitchcock, S. A. Holmes, M. F. Lappert, *J. Chem. Soc. Dalton Trans.* **1995**, 1435–1440; d) A. G. Avent, M. A. Edelmann, M. F. Lappert, G. A. Lawless, *J. Am. Chem. Soc.* **1989**, *111*, 3423–3425.
[33] G. B. Deacon, C. M. Forsyth, *Chem. Eur. J.* **2004**, *10*, 1798–1804.
[34] a) M. Veith, J. Böhnlein, V. Huch, *Chem. Ber.* **1989**, *122*, 841–849; b) P. C. Andrews, D. R. Baker, R. E. Mulvey, W. Clegg, P. O'Neil, *Polyhedron* **1991**, *10*, 1839–1841.
[35] a) From a survey of the Cambridge Structural Database. b) M. L. Cole, D. J. Evans, P. C. Junk, M. K. Smith, *Chem. Eur. J.* **2003**, *9*, 415–424.
[36] R. D. Shannon, *Acta Crystallogr. Sect. A* **1976**, *32*, 751–767.
[37] M. Wedler, M. Noltemeyer, U. Pieper, H.-G. Schmidt, D. Stalke, F. T. Edelmann, *Angew. Chem.* **1990**, *102*, 941–943; *Angew. Chem. Int. Ed. Engl.* **1990**, *29*, 894–896.
[38] G. B. Deacon, C. M. Forsyth, N. M. Scott, B. W. Skelton, A. H. White, *Aust. J. Chem.* **2001**, *54*, 439–446.
[39] a) M. Sotoodeh, I. Leichtweis, H. W. Roesky, M. Noltemeyer, H.-G. Schmidt, *Chem. Ber.* **1993**, *126*, 913–919; b) F. Perdih, A. Pevec, S. Petriček, N. Lah, K. Kogei, A. Damšar, *Inorg. Chem.* **2006**, *45*, 7915–7921.
[40] a) A. Herzog, H. W. Roesky, Z. Zak, M. Noltemeyer, *Angew. Chem.* **1994**, *106*, 1035–1037; *Angew. Chem. Int. Ed. Engl.* **1994**, *33*, 967–968; b) A. Herzog, H. W. Roesky, F. Jäger, A. Steiner, M. Noltemeyer, *Organometallics* **1996**, *15*, 909–917.
[41] G. B. Deacon, G. Meyer, D. Stellfeldt, *Eur. J. Inorg. Chem.* **2000**, 1061–1071.
[42] a) E. A. Fedorova, N. V. Glushkova, M. N. Bochkarev, H. Schumann, H. Hemling, *Izv. Akad. Nauk Ser. Khim.* **1996**, 2101–2104; b) R. A. Andersen, T. D. Tilley, C. J. Burns, *J. Chem. Soc. Chem. Commun.* **1984**, 710–711.
[43] a) G. B. Deacon, C. M. Forsyth, D. L. Wilkinson, E. T. Lawrenz in *Synthetic Methods of Organometallic and Inorganic Chemistry, Vol. 6* (Ed.: W. A. Herrman), Theime, NewYork, **1997**, pp. 48–51; b) R. Johnson, W. L. McEwan, *J. Am. Chem. Soc.* **1926**, *48*, 469–478; c) J. L. Namy, P. Girard, H. B. Kagan, P. E. Caro, *Nouv. J. Chim.* **1981**, *5*, 479–484.
[44] a) R. H. Blessing, *J. Appl. Crystallogr.* **1997**, *30*, 421–426; b) G. M. Sheldrick, SADABS: Program for scaling and absorption correction of area detector data, Universität Göttingen, **1997**; c) G. M. Sheldrick, *Acta Crystallogr. Sect. A* **2007**, *64*, 112–122; d) L. J. Barbour, *J. Supramol. Chem.* **2001**, *1*, 189–191.

Received: November 5, 2008
Published online: February 16, 2009

